



Analysis of Karst Surface Anisotropy Using Directional Semivariograms, Slovenia

TIMOTEJ VERBOVŠEK¹

Abstract—The paper presents a study of the anisotropic properties of the karst surface through the use of semivariograms. Karst is formed by hydrogeological and tectonic deformations that determine the surface and subsurface characteristics of the area. Among the most prominent surface features are dolines, which generally form in a linear direction. Semivariograms can be used to determine both the preferred direction of anisotropy and the degree of anisotropy. The surface exhibits the greatest elevation variability in the direction of the most diverse terrain, corresponding to dolines. The results, based on the eight karst areas studied, show that it is possible to detect and, more importantly, quantify anisotropy in all karst areas, although in some cases it is impossible or difficult to detect visually. The directions of the semivariograms agree very well with those obtained from the visual inspection of the maps, as well as with the orientations of the main faults. The method is therefore very useful for quantitative determination of anisotropy and its interpretation could be greatly improved by using the detailed structural geological maps of the karst.

Keywords: Karst, dolines, anisotropy, semivariogram, surface variability, Slovenia.

1. Introduction

The influence of tectonics on karst morphology and quantitative geomorphological approaches were recognized early in karst research (Evans, 1972; Jennings, 1975; White & White, 1979; Williams, 1972a, 1972b) and the influence of faults on carbonate relief and karst hydrology is a well-known fact (Ford & Williams, 2007). Among the most studied karst features are dolines, and although they are obvious geomorphological objects, their origin and even delineation are still problematic (Basso et al., 2013; Bauer, 2015; Bondesan et al., 1992; Denizman, 2003; Evans, 2012; Ford & Williams, 2007; Sauro,

2003; Šegina et al., 2018; Verbovšek & Gabor, 2019). Dolines are usually not randomly distributed in space, but follow tectonic structures, mostly faults and fracture zones which generally determine karstic topography and hydrogeology (Bauer et al., 2016; Čar, 1982, 1986, 2001, 2018; Mihevc & Mihevc, 2021; Šušteršič, 2002, 2006; Žvab Rožič et al., 2015).

Located at the junction of the Pannonian Basin, the Alps, and the Adriatic Sea, Slovenia has a strong topographic relief and a diverse geological setting (Fig. 1). One of the most known geological characteristics of Slovenian landscape is karst. This term was originally named after the Slovenian geographic region Kras (Classical karst, a carbonate plateau located between the Gulf of Trieste in the west and the Friulian plain in the northwest), and consequently this term Kras entered the world terminology in its equivalent German form *Karst*. Classical karst is part of the Dinaric karst, a well-studied region that extends from Slovenia through Croatia, Bosnia and Herzegovina (Fig. 1a), and further towards the southeast through Montenegro into Albania (Ford & Williams, 2007; Mihevc et al., 2010). About 43% of the area of Slovenia is composed of karst rocks, 8% of which are dolomites (Gams, 2004), and these karst rocks cover mainly the alpine NW part of the country, the Dinaric carbonate mountains and hills in the SE and SW and occur only as isolated karst patches in the north-eastern areas towards the Pannonian Basin. Carbonates formed almost continuously over a long period of time, with the oldest limestones in the Devonian, and later continuously from the Upper Permian through entire Mesozoic and some isolated limestones in the Miocene (Ogorelec, 2011; Ogorelec et al., 2000). The almost continuous deposition of carbonates has resulted in a sequence of carbonates over 7 km thick, with very different sedimentological

¹ Faculty of Natural Science and Engineering, University of Ljubljana, Aškerčeva 12, 1000 Ljubljana, Slovenia. E-mail: timotej.verbovsek@ntf.uni-lj.si

and hydrogeological characteristics (Verbovšek, 2008; Verbovšek & Veselič, 2008).

Because of this variety of different carbonates and the existence of large areas of karst rocks, the Slovenian territory is very suitable for the study of karst. The focus of the work is on the study of the anisotropy of the karst surface, which corresponds to the tectonic elements. We have used surface morphology to analyze the effects of anisotropy using directional semivariograms. Consequently, when the surface is flat, it is isotropic. However, the karst surface often has multiple dolines that may be visually randomly distributed in space. As mentioned earlier, dolines often appear in a linear direction corresponding to the direction of the fault or fracture zone, and the variability of the doline-pitted surface can be quantified.

Karst anisotropy can be of great help in studying the initiation and evolution of the karst area, which is

usually determined by structural mapping of the karst (Čar, 1982, 2001, 2018; Žvab Rožič et al., 2015). These data can then be used for further hydrogeological studies by correlating the determined directions with groundwater flow directions. However, this is not always directly possible because groundwater flow is affected by changes in rock conductivity, as tectonic deformation affects karst rocks very differently—their groundwater conductivity can either increase or decrease in different tectonic zones, and such complex behavior can even occur in the same fault (Bauer et al., 2016; Caine et al., 1996; Čar, 1982). Groundwater is often deflected from its general direction (gradient) and directed into so-called collecting channels by deflection faults (Šušteršič, 2002, 2006). Consequently, the locations of karst springs can also be associated with the direction of groundwater flow, and the actual flow of water can be confirmed by tracer tests (unfortunately, such

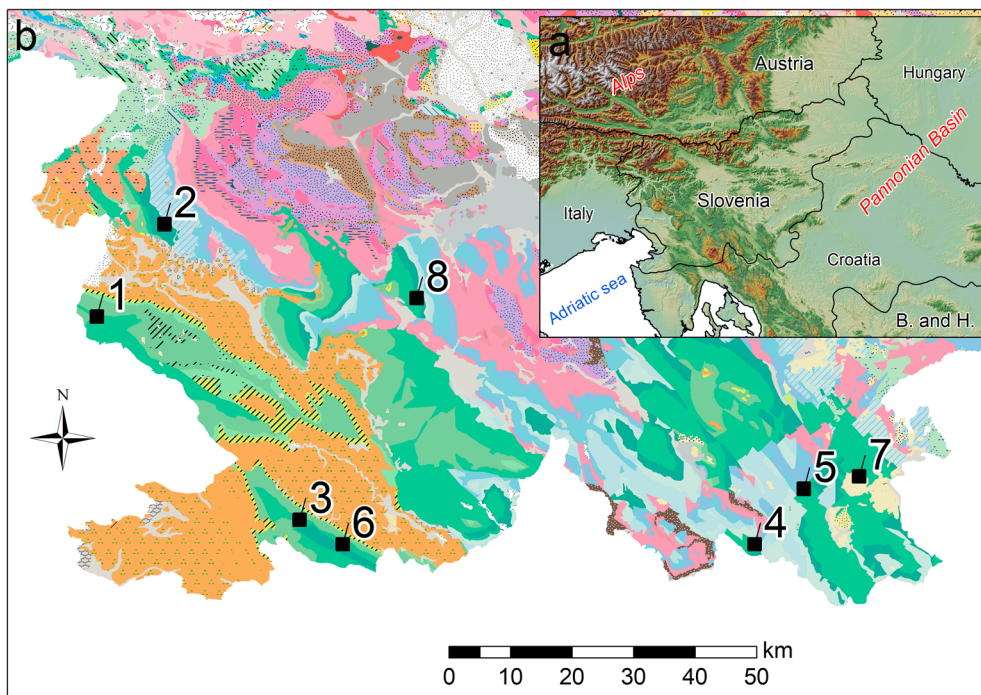


Figure 1

a Inset of Slovenia, **b** Lithological map (scale 1:250,000) showing study areas (Buser & Komac, 2002). Simplified legend for the southern part of the country in chronological order: Dark brown: Permian clastic rocks. Pink and purple: triassic limestones, dolomites and to a lesser extent clastic and volcanic rocks. Blue: mostly Jurassic limestones and dolomites. Green: Cretaceous limestones and to much lesser extent dolomites. Orange: paleocene and eocene flysch (alteration of mostly sandstones and marlstones). Gray: quaternary clastic sediments, mainly gravel. Numbers 1–8 represent the numbers of the studied areas in the text. B. and H.: Bosnia and Herzegovina. Source of Fig. 1a elevations: SRTM data (Jarvis et al., 2008)

confirmations are beyond the scope of this study). Since such deflection faults may be overlooked during mapping, the orientation of the dolines and the determined anisotropy direction of their orientation can be of great help in the analysis of the karst terrain, either for the study of the tectonic evolution of the area or for hydrogeological research (tracer tests, water supply and contamination studies). The anisotropy direction could be combined with the directional studies of landscape wavelengths commonly studied with single or double Fourier analyses (Brook & Hanson, 1991; Harrison & Lo, 1996; Podobnikar et al., 2019; Šušteršič, 1985), as these studies also recognize the spatial variation of different elevation wavelengths in different directions corresponding to faults and fracture zones in carbonates. In general, anisotropy can also be related to other surface roughness studies (see the work of Day & Chenoweth, 2013) where terrain properties can be quantified.

1.1. Geological Setting and Test Areas

The analyzed areas are all located in different types of Jurassic and Cretaceous limestones and, to a lesser extent, in dolomites and carbonate breccias. Other ages of carbonates were also considered for this study, but the selection of areas was severely limited by the spatial extent of the carbonates and also by the presence of dolines, which were necessary to conduct this study. A brief summary of the lithologic units is provided in Table 1.

2. Methods

2.1. Semivariogram Analysis

Surface anisotropy was studied using directional semivariograms to explore and interpolate spatial data. The semivariogram is a two-dimensional modeled plot that represents the dependence of the semivariance (one-half of the variance) of the surface elevation on the distance between pairs of sampled points. In general, the closer the points are to each other, the lower the variance (semivariogram) of elevation (Liang & Xu, 2014). It therefore represents

the spatial variability and also a 'roughness' of the data, which is one of the main components of general geomorphometry and is a function of relative surface relief (Day & Chenoweth, 2013). The curve of the semivariogram is fitted to the data using various semivariogram models, and its shape is modeled by a mathematical function. Variograms usually provide insight into the spatial statistics of the data and are typically used in kriging to model spatial variability (Davis, 2002). However, they can also be used to study anisotropy by examining the different semivariograms in different directions, but such studies are much rarer, especially in karst (Day & Chenoweth, 2013). Notable exceptions include the study of the use of variograms to determine fractal dimensions of terrain (McClellan & Evans, 2000), the study of the surface morphology of scree slopes (Trevisani et al., 2009), the tectonic interpretation of the Amazonian landscape (Ibanez et al., 2014) and the research most relevant to karst, i.e., the study of tower and cockpit karst (Liang & Xu, 2014), the study of cockpit karst in Jamaica (Lyew-Ayee et al., 2007), and that of Pardo-Igúzquiza et al. (2016) for the morphometric analysis of karst channels, the latter two using the directional semivariograms.

Analysis of directional semivariograms was performed in ArcGIS 10.5.1 software under the Geostatistical Analyst package (Johnston et al., 2001) using the Geostatistical Wizard. In this study, the stable semivariogram model was used, as it fitted the data better than the linear, Gaussian, exponential, or spherical models. The spherical semivariogram model flattens faster and therefore was not applicable to the data used. The linear semivariogram model is also not suitable because it has a stable slope. Among the other models, the spherical, exponential, Gaussian, and stable semivariogram models were found to be the most appropriate, and it was decided to use the stable semivariogram model because it was the best fit to the experimental data. The goodness of fit curves was determined both by numerically examining the errors in the final step of semivariogram modeling in ArcMap Geostatistical Analyst and by visually assessing the fit curves with the experimental data, since for some areas the fit was good for some semivariogram models but the fitting curve deviated a lot for an area of two. Therefore, a combination of

Table 1
Studied areas and their geological properties

Area No.	Short name	Geological setting	Visual anisotropy estimation	Range ratio	St. dev. (m)	Azimuth (semivariogram), red in Fig. 2	Azimuth (manual), Azimuth (BGM), green in Fig. 2	Azimuth (BGM), blue in Fig. 2
1	Kras	Lower- and upper-Cretaceous limestones and dolomites, upper Cretaceous limestones with rudists Thick-bedded micritic limestone and bituminous dolomite (Lower Cretaceous and lower part of upper Cretaceous) Rudist and micritic limestone—Sežana formation Upper Cretaceous—turonian	Low/no anisotropy	1.41	10.7	65°	No	No
2	Tnovo	Bedded lower Cretaceous limestones, lower Cretaceous oolitic limestones, upper jurassic coral limestones Alternation of limestone and dolomite (lower part), micritic limestone (upper part) Lower Cretaceous—Berriasian-Barremian Reef limestone with corals, hydrozoans and sponges Lower part of upper Jurassic—lower Kimmeridgian-Oxfordian	High anisotropy in two directions	1.41	32.7	10°	15°	10°
3	Matarsko podolje	Lower- and upper-Cretaceous limestones and limestone and dolomite breccias, upper Cretaceous limestones with rudists Thick-bedded micritic limestone and bituminous dolomite Lower Cretaceous and lower part of upper Cretaceous Rudist and micritic limestone—Sežana formation Upper Cretaceous—Turonian	High anisotropy	2.71	11.6	130°	120°	115°
4	Bilpa	Biomicritic lower Cretaceous limestones, and to a lesser extent dolomites, limestone breccias and upper Jurassic limestones Thick-bedded micritic limestone and bituminous dolomite Lower Cretaceous and lower part of upper Cretaceous Alternation of limestone and dolomite (lower part), micritic limestone (upper part)	High anisotropy	1.77	32.6	150°	155°	150°
5	Rog	Lower Cretaceous—Berriasian-Barremian Lower Cretaceous biomicritic limestones, mid Jurassic micritic limestones, and to lesser extent lower Jurassic dolomites Thick-bedded micritic limestone and bituminous dolomite Lower Cretaceous and lower part of upper Cretaceous Micritic and oolitic limestone, bituminous dolomite Upper Lias-Dogger	High anisotropy in two directions	1.32	64.0	15°	15°	40°
6	Podgrad	Lower Cretaceous limestones, limestone breccias and dolomites Alternation of limestone and dolomite (lower part), micritic limestone (upper part) Lower Cretaceous—Berriasian-Barremian Thick-bedded micritic limestone and bituminous dolomite Lower Cretaceous and lower part of upper Cretaceous	High anisotropy	1.87	33.6	115°	120°	No

Table 1 continued

Area No.	Short name	Geological setting	Visual anisotropy estimation	Range ratio	St. dev. (m)	Azimuth (semivariogram), red in Fig. 2	Azimuth (manual), Azimuth (BGM), green in Fig. 2 blue in Fig. 2
7	Gradac	Lower Cretaceous micritic limestones, limestone breccias Thick-bedded micritic limestone and bituminous dolomite Lower Cretaceous and lower part of upper Cretaceous	Low/no anisotropy	1.92	6.8	120°	30°, 115° 40°, 135°
8	Ravnik	Lower and upper Cretaceous limestones and dolomites, to a lesser extent upper Jurassic dolomites Thick-bedded micritic limestone and bituminous dolomite Lower Cretaceous and lower part of upper Cretaceous Alternation of limestone and dolomite (lower part), micritic limestone (upper part) Lower Cretaceous—Berriasian-Barremian	Low anisotropy	1.97	17.8	135°	140° No

BGM: Basic Geological Map 1:100,000. All azimuths are rounded to 5°

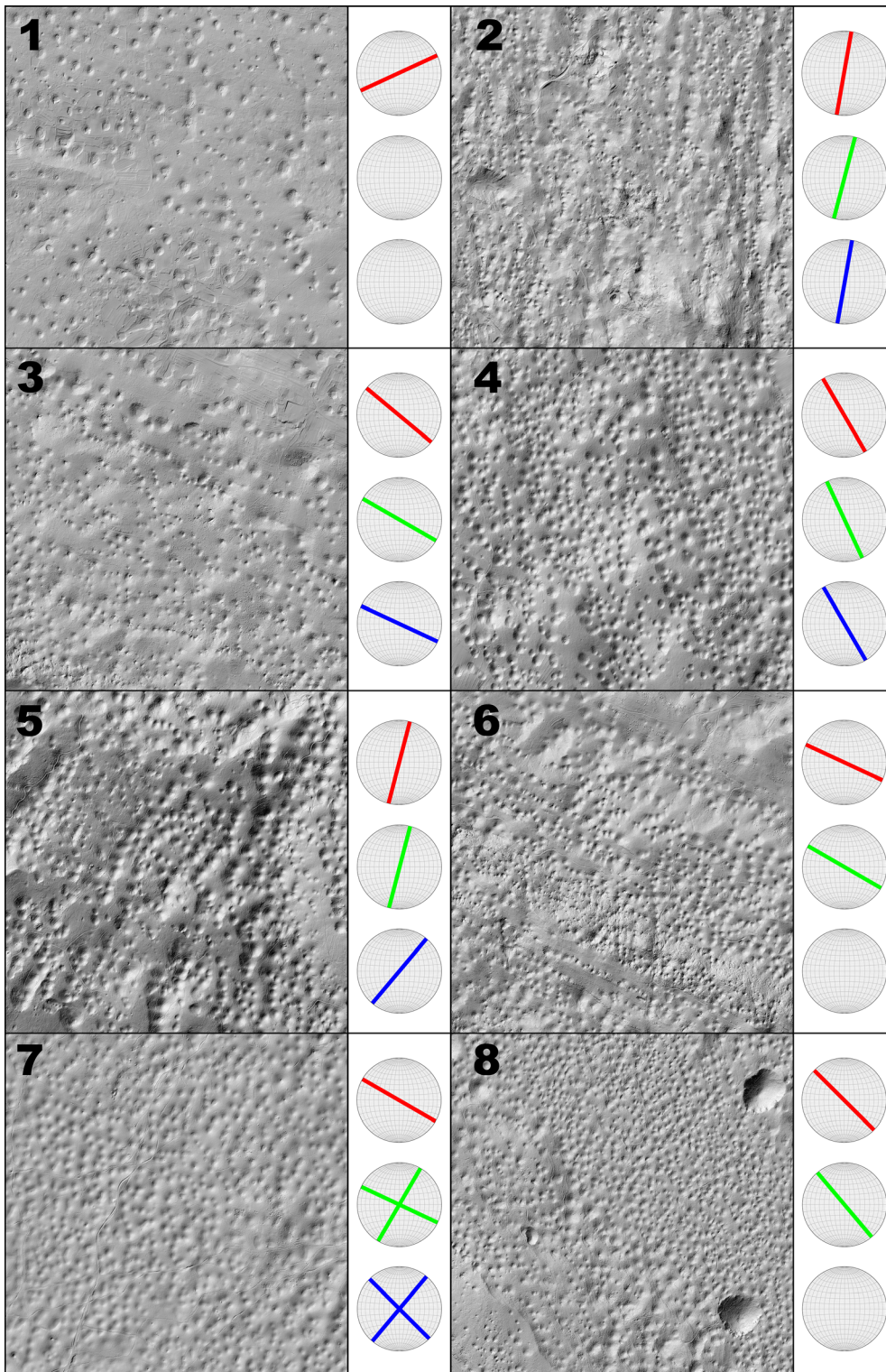
both approaches was preferred. In addition, the stable semivariogram model used is only a variation of the exponential semivariogram model (Johnston et al., 2001) with an exponent in the range between 0 and 2, unlike the exponential semivariogram model which has a fixed exponent of 1, so the advantage of the stable semivariogram model is that it can be fitted to data with larger variations. The spherical semivariogram model was only slightly worse at fitting the curve to experimental data. In fact, there is no agreement on the preferred semivariogram model in the literature cited, as a K-Bessel model was used in the study by (Ibanez et al., 2014), the logarithmic model was used in the study by (McClellan & Evans, 2000), and the spherical model was used in the study by (Lyew-Ayee et al., 2007). The choice of model clearly depends on the shape of the experimental data. Some approaches even use manual estimation of the values using a visual subjective choice of the linear fit of the logarithmic semivariograms ((McClellan & Evans, 2000).

Stable semivariogram model is defined as (Johnston et al., 2001):

$$\gamma(h; \theta) = \theta_s \left[1 - \exp\left(-\frac{3\|h\|}{\theta_r}\right) \right] \text{ for all } h$$

where θ_s is the partial sill parameter and $\theta_r \geq 0$ is the range parameter.

The usual results of the semivariogram are the range, nugget, and sill values (Barnes, 2024; Johnston et al., 2001). Range is defined as the distance at which the model curve flattens, *nugget* represents the intercept value on the y-axis, and *sill* is the value at which the model first flattens out. These three values are usually intensively studied and defined when the goal of the research is to interpolate the data for further study and to compare kriging with other methods (e.g., IDW, spline, and others; Johnston et al., 2001). However, two other important results are calculated when examining anisotropy. The first is the ratio between the major and minor values of the range. This ratio is equal to one for isotropic surfaces and increases with increasing anisotropy. The second is the direction of the major axis, which is the azimuth of the highest surface variability. If dolines appear in a linear direction, the surface in that direction has the greatest variability and consequently



◀Figure 2

Hillshaded digital elevation models of studied areas. Numbers correspond to the area numbers (Table 1). Red directions correspond to semivariogram directions, green to manual directions and blue to major fault directions (values are presented in Table 1)

can be used for comparison with the direction of the faults. The graphical representation of anisotropy can also be studied using the semivariogram curves, which are set off at 10° intervals from the determined most anisotropic direction. When the surface is isotropic, all the semivariogram curves overlap (all are equal), and in the case of high anisotropy, the curves are more separated.

The anisotropy detection workflow is defined in the Geostatistical Analyst package (Johnston et al., 2001). Prior to using this package, the lidar surface, used in this study and described below in Sect. 2.2, was transformed from a raster to a vector point layer because the kriging in Geostatistical Analyst requires point data for interpolation. In the first step, the kriging method was used with Ordinary kriging since the mean is unknown. The second step involves semivariogram modeling where anisotropy was defined along with all semivariogram parameters. This step is crucial for the detection of anisotropy, as the smaller and larger range and the direction angle are read out. The other steps 3 and 4 represent Searching neighborhood and Cross correlation, which are not used for anisotropy analyzes. The determined angle directions and minor/major ranges were then entered into the table and figures for comparison with the fault directions obtained from the geologic maps.

2.2. Elevation Data

For our study, we used a high-resolution (1×1 m) digital elevation model (DEM) of Slovenia obtained by laser scanning (lidar) in 2014–2015 (ARSO, 2014). Scanning was performed using a Riegl LMS-Q780 scanner, with vertical accuracy estimated at about 2.5 cm (between 1.5 cm and 2.5 cm). Horizontal accuracy is between 1.5 cm and 2.0 cm in both N-S and E-W directions. The raster elevations were converted into a vector layer of 1×1 m points used for geostatistical analysis

(kriging). Eight areas of 2×2 km size were tested. The choice of this area size was limited by the computational limits of the software and the limits of the lithological units, since the analyzed map should include only the karstic terrain preferably within one lithological unit.

Larger areas would be more suitable, because the flattening of semivariograms would be better visible, thus the ranges would be larger. However, two problems arise with the incrementation of the area size: first, the computational power of the computer decreases rapidly with the increased number of data (number of points), and for larger areas, it was impossible to calculate the semivariograms. Second problem is related to boundary conditions. By enlargement of the areas, different geological structures are encountered, so the surface morphology changes rapidly in different geological setting, and it is not possible anymore to perform the analyses. Regarding the smaller areas (1×1 km), this would be possible, but then the number of data for the semivariogram analysis would quickly decrease, and this would implement also the lower quality of the results. More importantly, with smaller areas it would be quickly possible to miss the dolines appearing in any direction, so the anisotropy effects would be missed.

3. Results and Discussion

The highest anisotropy is seen in the limestones of Matarsko podolje (area No. 3) with a ratio of major and minor axis of 2.71 (Table 1). The direction determined from the semivariogram is 130° , which is very similar to both the visual assessment of the “doline chain” in the hatched map and the azimuth of the faults (120°) in the geological map (115° , Table 1). The anisotropic surface is also evident from visual inspection (Fig. 2). The curves of the semivariograms are far apart (Fig. 3), indicating quite different statistical properties of the surface in different directions.

Another site in a similar geological setting with high anisotropy is the Podgrad region (area No. 6), where the ratio is 1.87. Despite the higher visual anisotropy (clearer direction of dolines), the ratio is

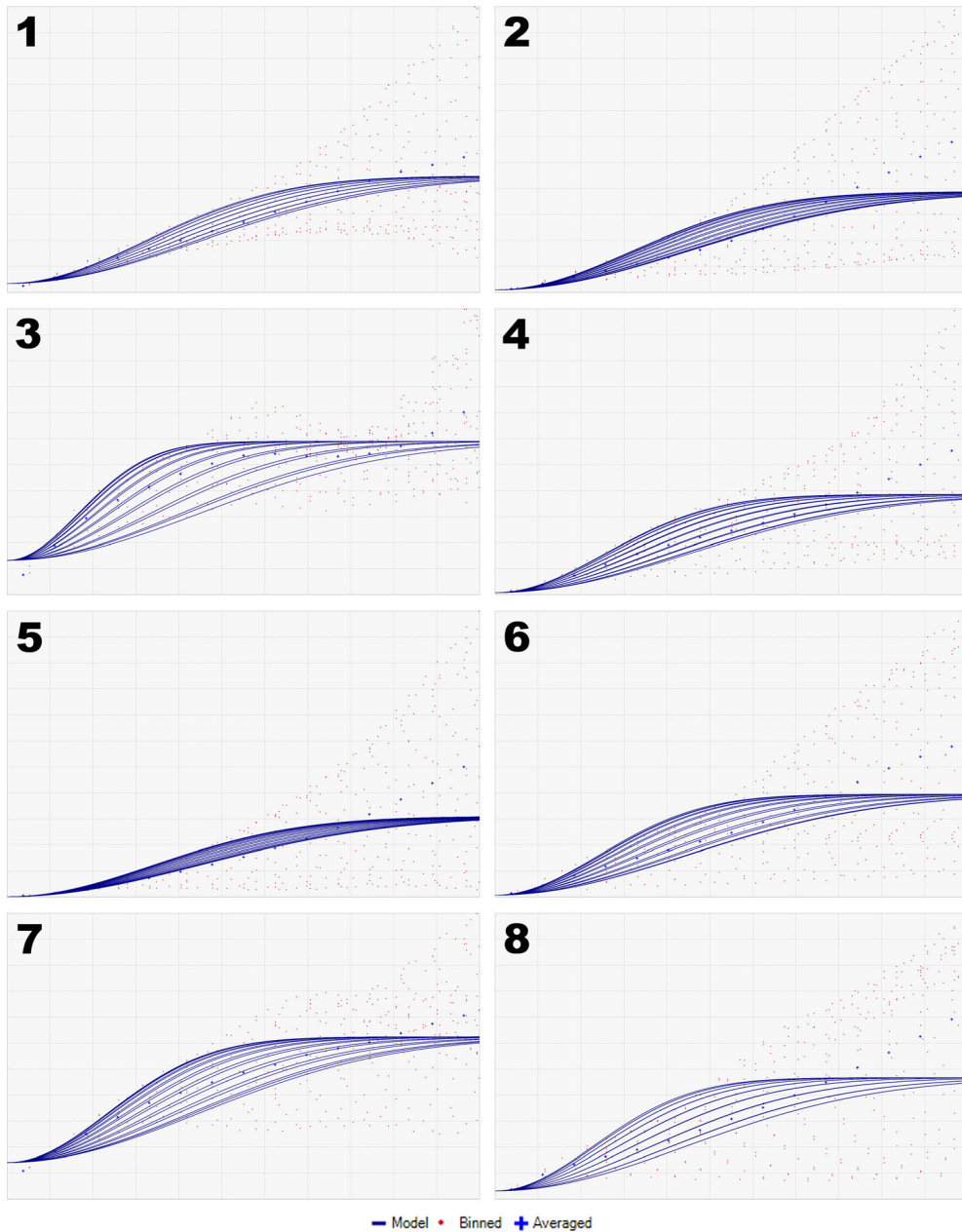


Figure 3

Semivariograms of the areas studied. The numbers correspond to the numbers of the areas (Table 1). For comparison, the distance on the x-axis is the same for all semivariograms (1500 m), the maximum value of semivariance on the y-axis is different for the regions, as follows: ①: 320 m, ②: 3129 m, ③: 251 m, ④: 3041 m, ⑤: 14,000 m, ⑥: 3217 m, ⑦: 90 m, ⑧: 768 m

lower than in the earlier area (no. 3), which is most likely due to the larger standard deviation of the surface elevation (Table 1). The Matarsko podolje area has a standard deviation three times lower than

the Podgrad region, which leads to a more recognizable automatic anisotropy. The visual estimate of the direction of the main doline is almost identical to that obtained from the semivariogram, and there is

only one preferred direction. There is no preferred direction of the faults on the geologic map for comparison.

Area No. 7 (Gradac) appears contradictory when comparing visual anisotropy and numerical results. The visual inspection shows two doline directions, but they are not very clear and the area ratio is very high (1.92). This contradictory fact can be attributed to a very low standard deviation of the elevations, which is the lowest of all studied areas (6.8 m). Dolines are therefore better detected than at the other sites and anisotropic effects are more pronounced. Similar to the previous region, there is no preferred direction of faults on the geologic map.

A similar discrepancy, but not as obvious, applies to area No. 8 (Ravnik). The range ratio is the second highest (1.97), but the anisotropy is more evident on the hillshaded surface. The standard deviation is also much higher (17.8 m) than in the Gradac region. The visual estimate of the direction of the main doline is almost identical to that obtained from the semivariogram. Similar to the other two regions, there is no preferred direction of the faults on the geological map.

The Bilpa area (No. 4) is the last among the regions with a high range ratio and has a ratio of 1.77. The visual orientation is very clear and perfectly coincides with the fault direction determined from the geological map. However, the ratio is lower than in the previously described regions, probably due to the higher standard deviation of the elevations (32.6 m).

The lowest ratio appears in the Rog area (No. 5), which has the highest standard deviation of elevations (64 m). Visual anisotropy is evident, and the visual direction of the dolines is almost corresponds to the direction determined from the semivariogram. The direction of the faults on the geologic map deviates slightly, about 35°. However, the ratio is quite low, which can be attributed to the highest standard deviation of the elevations, which obscures the recognition of doline orientations and anisotropy calculations. The curves of the semivariogram (Fig. 3) are the closest of all semivariograms.

For the Kras region (area No. 1), no anisotropy is evident, neither from the visual assessment nor from the geological map, however the semivariogram shows a direction of 65°. The standard deviation of

the elevations is very low and range ratio is 1.41, the second lowest for all regions. Therefore, the very small anisotropic effects are a reliable conclusion.

The same range ratio (1.41) appears in the Trnovo area (No. 2). Similar to the Rog area (no. 5), the visual anisotropy is high, even in two directions, and the visual directions agree very well with those from the semivariogram and those from the geological map. Nevertheless, the ratio is very low and the semivariogram curves are very close (Fig. 3). This discrepancy can be attributed to a rather high standard deviation of the elevations, which obscures the detection of doline alignments.

The above directions (azimuths) were also compared with the general directions of the water tracer tests carried out in Slovenia between 1905 and 2019. The GIS database was compiled from more than 200 tracer tests (Petrič et al., 2020), which were already documented in 1946, 1989 and 1990 (Petrič, 2009). The directions were taken from the GIS data layer “Groundwater connections”, which shows the connections between the injection points and the sampling points of the tracer tests. It is important to note that these connections are linear and were determined by simple GIS connections between two points, so they do not represent the actual pathways of the groundwater.

Due to the problems with very simplified (average) groundwater directions and the fact that the studied areas are consequently crossed by numerous water flow directions, a general comment is given for each area and no numerical indication is given for each of the numerous tracer directions. In general, for half of the areas, the agreement between the tracer test direction and the directions of the major faults, the semivariogram and the manual directions is moderate to good (areas no. 3, 4, 5 and 6, Fig. 4). The problem is that in most regions there are several groundwater flow directions due to the bifurcation of groundwater flow in the karst. In some regions the “groundwater connections” do not cross the investigated areas or there is only one connection (areas 1, 2, 7), so that a comparison is not possible. For area no. 8, most of the groundwater directions are to the north, but the orientation of dolines and faults is not similar. Thus, despite the initial “tempting” idea of using the directions of the tracer tests, a comparison

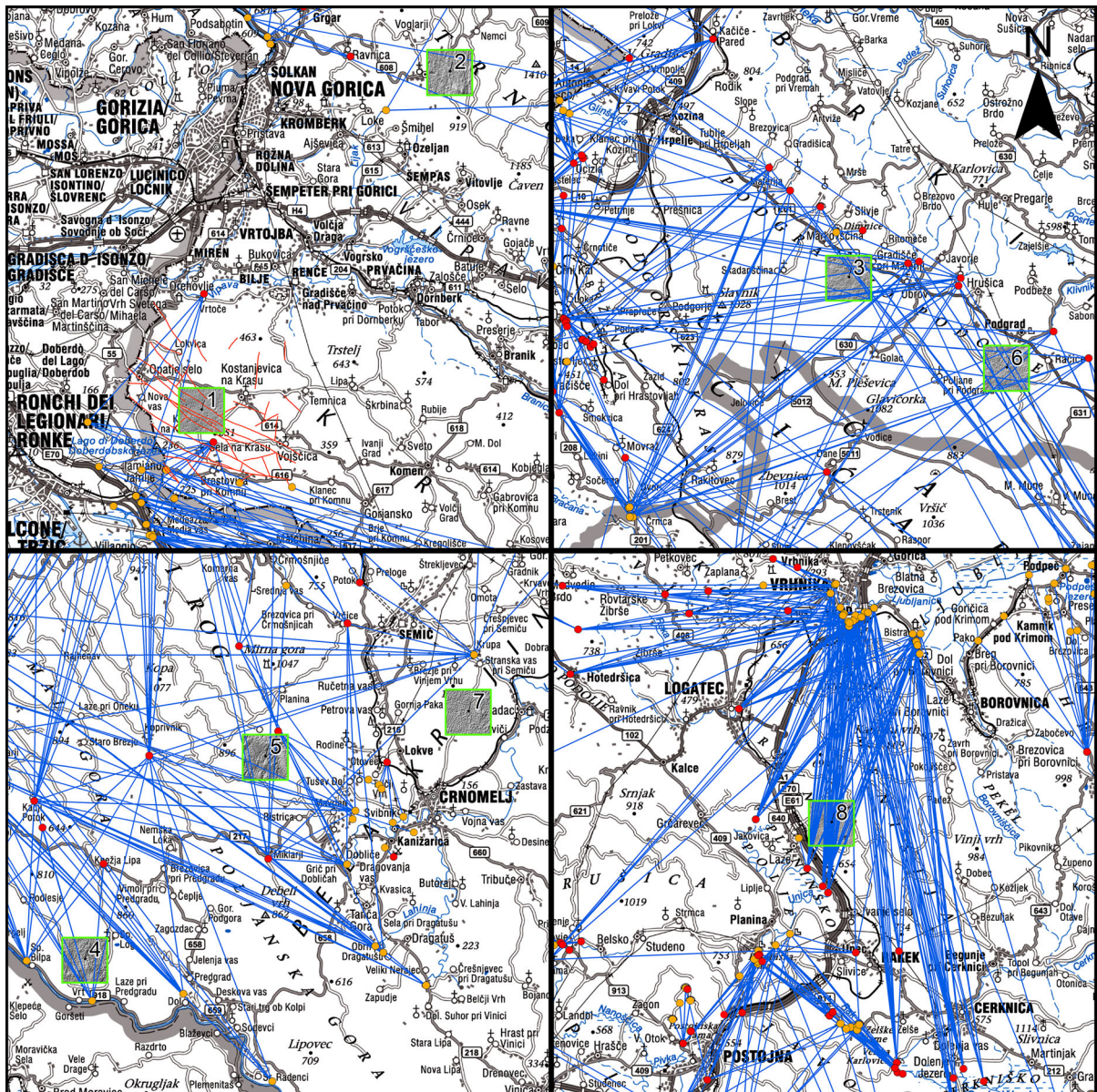


Figure 4

Groundwater connections of the tracer test database for the studied regions. The extent of all four regions is 24×24 km. Source of the tracer test data: Petrič et al., 2020. Source of topographic data: The Surveying and Mapping Authority of the Republic of Slovenia, Topographic map 1:250,000)

with the directions of the main faults, the semivariogram and the manual directions of the dolines is unfortunately not useful. The reason for the poor agreement is, as mentioned in the “Introduction” section, that the groundwater is often deflected from its general direction (Šušteršič, 2002, 2006) along the tectonic elements.

4. Conclusions

The anisotropy of the karst surface is very pronounced and the dolines occur in preferential directions. An important fact is the recognition of anisotropy by the semivariogram method in the areas that are visually isotropic or where it is difficult to

detect the anisotropy visually. Most importantly, anisotropy can be quantified by identifying two factors: first, the preferred direction of the most varying surface elevation, and second, the variability of elevations in those directions.

Using only the semivariogram curve analysis or the ratio between the major and minor ellipse axes is not recommended, as all results should be analyzed by combining the visual approach and the analysis of fault directions. The variation of the standard deviation of the surveys is also an important factor as it affects the variation of the results, and it is known that data variability has a negative impact on the performance of spatial interpolation methods (Li & Heap, 2014), and high values of standard deviation indicate a higher degree of uncertainty (Trevisani et al., 2009). The lower the standard deviation, the more reliable the conclusions about the anisotropic properties of the studied surface. The method is not only suitable for areas with low topographical relief (plains), as the areas with lower standard deviation can also occur at higher altitudes (e.g. a karst plateau).

The preferred directions agree very well with the manually estimated directions of doline alignments and main fault directions from the geological maps. The “manually estimated directions” were drawn according to the existing fault traces on the geological maps, so that no subjective factor influenced the direction. However, it should be noted that the scale taken for estimation of fault directions was 1:100,000 scale, which is not directly suitable for the 2×2 km areas studied. The problem is the lack of more detailed systematic geological maps. For the area of Kras (No. 1), the map exists at the scale of 1:25,000, but consequently the results would not be comparable with other regions if all other areas had a different scale. Also, the map is available only for this region, and only in a printed form, which consequently would have had to be manually georeferenced, leading to errors in both location and rotation of the spatial data. An appropriate and proposed solution (but beyond the scope of this study) would be detailed structural-geological mapping at finer scales, which would determine not only the more precise location and number of faults, but also the different types of fault zones that influence the formation and development

of dolines. In Slovenia, there are few examples of such mapping (pioneering work in structural geological mapping by Breg Valjavec et al., 2022; Čar, 1982, 1986, 2001, 2018; Šebela, 1998; Vrviščar, 2016; Žvab Rožič et al., 2015), although these published works cover different areas than those in our study. Future work will therefore focus on the study of surface anisotropy in combination with detailed structural-geological mapping and karst surface necessary for understanding the evolution of the karst surface. The determined directions of the dolines could also be used for further hydrogeological investigations by correlating the determined directions with detailed groundwater flow directions. As mentioned above, there is a large GIS database of tracer tests conducted in Slovenia (231 tracer tests; Petrič et al., 2020), but a comparison does not provide useful results due to the very simplified groundwater connections from the source to the tracer measurement points. Finally, groundwater flow is often diverted from the direction of the groundwater gradient and directed into collector channels, as evidenced by collapse doline studies (Šušteršič, 2002, 2006). Such deflection occurs due to changes in the hydrogeological properties of the rocks as a result of tectonic influences and the resulting karstification of the rocks (Čar, 1982). The only method to study these effects is detailed structural mapping of the above-mentioned area.

Acknowledgements

The author gratefully acknowledges financial support from the Slovenian Research Agency (Research Core Funding No. P1-0195 “Geoenvironment and Geomaterials”).

Author Contributions TV wrote the main manuscript text, prepared figures and tables.

Funding

This article is funded by Javna Agencija za Raziskovalno Dejavnost RS, P1-0195.

Data availability

Data cannot be shared openly but are available on request from authors.

Declarations

Conflict of interest The author has no relevant financial or non-financial interests to disclose.

Open Access This article is licensed under a Creative Commons Attribution 4.0 International License, which permits use, sharing, adaptation, distribution and reproduction in any medium or format, as long as you give appropriate credit to the original author(s) and the source, provide a link to the Creative Commons licence, and indicate if changes were made. The images or other third party material in this article are included in the article's Creative Commons licence, unless indicated otherwise in a credit line to the material. If material is not included in the article's Creative Commons licence and your intended use is not permitted by statutory regulation or exceeds the permitted use, you will need to obtain permission directly from the copyright holder. To view a copy of this licence, visit <http://creativecommons.org/licenses/by/4.0/>.

Publisher's Note Springer Nature remains neutral with regard to jurisdictional claims in published maps and institutional affiliations.

REFERENCES

- ARSO (2014) http://gis.arso.gov.si/evode/profile.aspx?id=atlas_voda_Lidar@Arso. Accessed 15 Sep 2022.
- Barnes R (2024) Variogram Tutorial. Golden Software Inc. <http://www.goldensoftware.com/variogramTutorial.pdf>. Accessed 15 Sep 2022.
- Basso, A., Bruno, E., Parise, M., & Pepe, M. (2013). Morphometric analysis of sinkholes in a karst coastal area of southern Apulia (Italy). *Environmental Earth Sciences*, 70, 2545–2559. <https://doi.org/10.1007/s12665-013-2297-z>
- Bauer, C. (2015). Analysis of dolines using multiple methods applied to airborne laser scanning data. *Geomorphology*, 250, 78–88. <https://doi.org/10.1016/j.geomorph.2015.08.015>
- Bauer, H., Schröckenfuchs, T. C., & Decker, K. (2016). Hydrogeological properties of fault zones in a karstified carbonate aquifer (Northern Calcareous Alps, Austria). *Hydrogeology Journal*, 24(5), 1147–1170. <https://doi.org/10.1007/s10040-016-1388-9>
- Bondesan, A., Meneghel, M., & Sauro, U. (1992). Morphometric analysis of dolines. *International Journal of Speleology*, 21(1–4), 1–55. <https://doi.org/10.5038/1827-806X.21.1.1>
- Breg Valjavec, M., Čiglič, R., Tičar, J., & Šebela, S. (2022). Determining the geomorphological and hydrogeological connections between dolines and the cave Polina peč using 3D laser scanning. *GIS v Sloveniji, Preteklost in prihodnost* (pp. 39–54). Ljubljana, Slovenia: ZRC SAZU Publishing house, Karst Research Institute. https://doi.org/10.3986/9789610506683_03
- Brook, G. A., & Hanson, M. (1991). Double Fourier series analysis of cockpit and doline karst near Browns town, Jamaica. *Physical Geography*, 12(1), 37–54.
- Buser, S., & Komac, M. (2002). Geological map of Slovenia 1:250,000. *Geologija*, 45(2), 335–340. <https://doi.org/10.5474/geologija.2002.029>
- Čar, J. S., Evans, J. P., & Forster, C. B. (1996). Fault zone architecture and permeability structure. *Geology*, 24(11), 1025–1028. [https://doi.org/10.1130/0091-7613\(1996\)024%3c1025:FZAAPS%3e2.3.CO;2](https://doi.org/10.1130/0091-7613(1996)024%3c1025:FZAAPS%3e2.3.CO;2)
- Čar, J. (1982). Geološka zgradba požiralnega obrobja Planinskega polja = Geologic Setting of the Planina Polje Ponor Area. *Acta Carsologica*, 10, 75–105.
- Čar, J. (1986). Geološke osnove oblikovanja kraškega površja = Geological bases of karst surface formation. *Acta Carsologica*, 24(25), 31–38.
- Čar, J. (2001). Structural bases for shaping of dolines. *Acta Carsologica*, 30(2), 239–256.
- Čar, J. (2018). Geostructural mapping of karstified limestones. *Geologija*, 61(2), 133–162. <https://doi.org/10.5474/geologija.2018.010>
- Davis, J. C. (2002). *Statistics and data analysis in geology*. Wiley.
- Day, M., & Chenoweth, S. (2013). Surface Roughness of Karst Landscapes. In J. Shroder & A. Frumkin (Eds.), *Treatise on Geomorphology, Karst Geomorphology* (Vol. 6, pp. 157–163). San Diego, USA: Academic Press.
- Denizman, C. (2003). Morphometric and spatial distribution parameters of karstic depressions, lower Suwannee River basin, Florida. *Journal of Cave and Karst Studies*, 65, 29–35.
- Evans, I. S. (1972). General Geomorphometry, Derivatives of Altitude and Descriptive Statistics. In R. J. Chorley (Ed.), *Spatial Analysis in Geomorphology* (pp. 17–90). London: Methuen.
- Evans, I. S. (2012). Geomorphometry and landform mapping: What is a landform? *Geomorphology*, 137(2012), 94–106. <https://doi.org/10.1016/j.geomorph.2010.09.029>
- Ford, D., & Williams, P. W. (2007). *Karst hydrogeology and geomorphology*. Chichester: Wiley. <https://doi.org/10.1002/9781118684986>
- Gams, I. (2004). *Kras v Sloveniji v prostoru in času*. Ljubljana, Slovenia: ZRC SAZU Publishing house, Karst Research Institute.
- Harrison, J. M., & Lo, C.-P. (1996). PC-based two-dimensional discrete Fourier transform programs for terrain analysis. *Computers & Geosciences*, 22(4), 419–424. [https://doi.org/10.1016/0098-3004\(95\)00104-2](https://doi.org/10.1016/0098-3004(95)00104-2)
- Ibanez, D. M., Miranda, F. P., & Riccomini, C. (2014). Geomorphometric pattern recognition of SRTM data applied to the tectonic interpretation of the Amazonian landscape. *ISPRS Journal of Photogrammetry and Remote Sensing*, 87, 192–204. <https://doi.org/10.1016/j.isprsjprs.2013.10.014>
- Jarvis A, Reuter HI, Nelson A, Guevara E (2008) Hole-filled seamless SRTM data V4, International Centre for Tropical Agriculture (CIAT). <https://srtm.csi.cgiar.org>. Accessed 24 Nov 2023
- Jennings, J. N. (1975). Doline morphometry as a morphogenetic tool: New Zealand examples. *New Zealand Geographer*, 31, 6–18. <https://doi.org/10.1111/j.1745-7939.1975.tb00793.x>
- Johnston K, Ver Hoef JM, Krivoruchko K, Lucas N (2001) Using ArcGIS geostatistical analyst. ESRI Press, Redlands, USA.

- http://downloads2.esri.com/support/documentation/ao/_Using_ArcGIS_Geostatistical_Analyst.pdf. Accessed 24 Nov 2023
- Li, J., & Heap, A. D. (2014). Spatial interpolation methods applied in the environmental sciences: A review. *Environmental Modeling & Software*, 53, 173–189. <https://doi.org/10.1016/j.envsoft.2013.12.008>
- Liang, F., & Xu, B. (2014). Discrimination of tower-, cockpit-, and non-karst landforms in Guilin, Southern China, based on morphometric characteristics. *Geomorphology*, 204, 42–48. <https://doi.org/10.1016/j.geomorph.2013.07.026>
- Lyew-Ayee, P., Viles, H. A., & Tucker, G. E. (2007). The use of GIS-based digital morphometric techniques in the study of cockpit karst. *Earth Surface Processes and Landforms*, 32, 165–179. <https://doi.org/10.1002/esp.1399>
- McClellan, C. J., & Evans, I. S. (2000). Apparent fractal dimensions from continental scale digital elevation models using variogram methods. *Transactions in GIS*, 4(4), 361–378. <https://doi.org/10.1111/1467-9671.00061>
- Mihevč, A., & Mihevč, R. (2021). Morphological characteristics and distribution of dolines in Slovenia, a study of a lidar-based doline map of Slovenia. *Acta Carsologica*, 50(1), 11–36. <https://doi.org/10.3986/ac.v50i1.9462>
- Mihevč, A., Prelovšek, M., & Zupan Hajna, N. (2010). *Introduction to the Dinaric Karst*. ZRC SAZU Publishing house.
- Ogorelec, B. (2011). Mikrofacies mezozojskih karbonatnih kamnin Slovenije. *Geologija*, 54(2), 1–136. <https://doi.org/10.5474/geologija.2011.011>
- Ogorelec, B., Dolenc, T., & Pezdič, J. (2000). Isotope composition of O and C in Mesozoic carbonate rocks of Slovenia - effect of facies and diagenesis. *Geologija*, 42, 171–205. <https://doi.org/10.5474/geologija.1999.012>
- Pardo-Igúzquiza, E., Pulido-Bosch, A., López-Chicano, M., & Durán, J. J. (2016). Morphometric analysis of karst depressions on a mediterranean karst massif. *Geografiska Annaler: Series a, Physical Geography*, 98(3), 247–263. <https://doi.org/10.1111/geoa.12135>
- Petrič, M. (2009). Review of water tracing with artificial tracers on karst areas in Slovenia. *Geologija*, 52(1), 127–136. <https://doi.org/10.5474/geologija.2009.013>
- Petrič, M., Ravbar, N., Gostinčar, P., Krsnik, P., & Gacin, M. (2020). GIS database of groundwater flow characteristics in carbonate aquifers: Tracer test inventory from Slovenian karst. *Applied Geography*, 118, 102191. <https://doi.org/10.1016/j.apgeog.2020.102191>
- Podobnikar T, Štefančič M, Verbovšek T (2019) A GIS-based approach to karst relief cyclicality by using Fast Fourier transform. AGILE 2019 – Limassol, June 17–20, 2019At: Limassol, Cyprus. https://agile-online.org/images/conference_2019/documents/short_papers/123_Upload_your_PDF_file.pdf. Accessed 24 Nov 2023
- Sauro, U. (2003). Dolines and sinkholes: Aspect of evolution and problems of classification. *Acta Carsologica*, 32(4), 41–52. <https://doi.org/10.3986/ac.v32i2.335>
- Šebela, S. (1998). *Tectonic structure of Postojnska jama cave system*. Ljubljana, Slovenia: ZRC SAZU Publishing house, Karst Research Institute. <https://doi.org/10.3986/961618265X>
- Šegina, E., Benac, Č., Rubinič, J., & Knez, M. (2018). Morphometric analyses of dolines – the problem of delineation and calculation of basic parameters. *Acta Carsologica*, 47(1), 22–33. <https://doi.org/10.3986/ac.v47i1.4941>
- Šušteršič, F. (1985). A method of doline morphometry and computer processing. *Acta Carsologica*, 13, 79–98.
- Šušteršič, F. (2002). Collapse dolines and deflector faults as indicators of karst flow corridors. *International Journal of Speleology*, 31, 115–127. <https://doi.org/10.5038/1827-806X.31.1.6>
- Šušteršič, F. (2006). Relationships between deflector faults, collapse dolines and collector channel formation: Some examples from Slovenia. *International Journal of Speleology*, 35, 11–12. <https://doi.org/10.5038/1827-806X.35.1.1>
- Trevisani, S., Cavalli, M., & Marchi, L. (2009). Variogram maps from LiDAR data as fingerprints of surface morphology on scree slopes. *Natural Hazards and Earth Systems Sciences*, 9, 129–133. <https://doi.org/10.5194/nhess-9-129-2009>
- Verbovšek, T. (2008). Diagenetic effects on the well yield of dolomite aquifers in Slovenia. *Environmental Geology*, 53(6), 1173–1182. <https://doi.org/10.1007/s00254-007-0707-9>
- Verbovšek, T., & Gabor, L. (2019). Morphometric properties of dolines in Matarsko podolje, SW Slovenia. *Environmental Earth Sciences*, 78, 396. <https://doi.org/10.1007/s12665-019-8398-6>
- Verbovšek, T., & Veselič, M. (2008). Factors influencing the hydraulic properties of wells in dolomite aquifers of Slovenia. *Hydrogeology Journal*, 16(4), 779–795. <https://doi.org/10.1007/s10040-007-0250-5>
- Vrviščar B (2016) Geological map of karst territory above the Medvedjak cave on the Matarsko podolje. Diploma work. University of Ljubljana, Faculty of Natural Sciences and Engineering. <https://repositorij.uni-lj.si/IzpisGradiva.php?lang=slv&id=87630>. Accessed 24 Nov 2023
- White, E. L., & White, W. B. (1979). Quantitative morphology of landforms in carbonate rock basins in the Appalachian Highlands. *Geological Society of America Bulletin*, 90, 385396. [https://doi.org/10.1130/0016-7606\(1979\)90%3C385:QMOLIC%3E2.0.CO;2](https://doi.org/10.1130/0016-7606(1979)90%3C385:QMOLIC%3E2.0.CO;2)
- Williams, P. W. (1972a). The Analysis of Spatial Characteristics of Karst Terrains. In R. J. Chorley (Ed.), *Spatial Analysis in Geomorphology* (pp. 135–163). Methuen.
- Williams, P. W. (1972b). Morphometric analysis of polygonal karst in New Guinea. *Geological Society of America Bulletin*, 83, 761–796. [https://doi.org/10.1130/0016-7606\(1972\)83\[761:MAOPKI\]2.0.CO;2](https://doi.org/10.1130/0016-7606(1972)83[761:MAOPKI]2.0.CO;2)
- Žvab Rožič, P., Čar, J., & Rožič, B. (2015). Geological structure of the Divača area and its influence on the speleogenesis and hydrogeology of Kačna jama. *Acta Carsologica*, 44(2), 153–168. <https://doi.org/10.3986/ac.v44i2.1958>